Systems & Control Transactions

Research Article - Peer Reviewed Conference Proceeding
ESCAPE 35 - European Symposium on Computer Aided Process Engineering
Ghent, Belgium. 6-9 July 2025
Jan F.M. Van Impe, Grégoire Léonard, Satyajeet S. Bhonsale,
Monika E. Polańska, Filip Logist (Eds.)

PSE PRESS

Machine Learning-Aided Robust Optimisation for Identifying Optimal Operational Spaces under Uncertainty

Sam Kay[a], Mengjia Zhu[a], Amanda Lane[b], Jane Shaw[b], Philip Martin[a], and Dongda Zhang[a]*

[a] Department of Chemical Engineering, University of Manchester, Manchester, M13 9PL, UK.
[b] Unilever R&D Port Sunlight, Bromborough Road, Bebington, Wirral, CH63 3JW, UK.
* Corresponding Author: dongda.zhang@manchester.ac.uk.

ABSTRACT

Process optimisation and quality control are crucial in process industries for minimising product waste and improving plant economics. Identifying robust operational regions that ensure both product quality and performance is particularly valued in industries. However, this task is complicated by operational uncertainties, which can lead to violations of product quality constraints and significant batch discards. We propose a novel robust optimisation strategy that integrates advanced machine learning and process systems engineering to systematically identify optimal operational regions under uncertainty. Our approach begins by using a process model to screen a broad operational space across various uncertainty scenarios, pinpointing promising control trajectories to satisfy process constraints and product quality. Machine learning is then employed to cluster these trajectories into sub-regions. Finally, a two-layer dynamic optimisation framework is employed to determine the optimal control trajectory and corresponding operable space within each promising sub-region. To demonstrate the efficiency of our approach, we used a case study focusing on the quality control of a dynamic batch process for formulation product manufacturing. The resulting operational regions were shown to meet product quality demands and offer a significant improvement in optimality over the current operation, highlighting the advantage and industrial potential of our strategy.

Keywords: Operational regions, Machine learning, Optimisation under uncertainty, Process control, Dynamic optimisation

INTRODUCTION

Product quality control is a critical concern in industries such as pharmaceuticals, speciality chemicals, and formulation processes, where strict regulatory standards are enforced to ensure safety, efficacy, and economic viability [1]. As a result, manufacturers face growing pressure to minimise product waste, a challenge particularly pronounced in pharmaceutical production, where batch rejections due to variability and quality deviations can result in significant economic and environmental consequences. To maintain a competitive edge while adhering to sustainability goals, there is a strong need for process optimisation strategies that enhance efficiency, reduce waste, and improve operational flexibility. Traditionally, process control has relied on rigid set-point strategies, where specific operating conditions are predetermined and maintained through fixed state profiles [2]. While effective in ensuring stable operations, such approaches lack adaptability in the face of uncertainty, making them prone to inefficiencies. Furthermore, the rigid nature of set-point control often results in excessive energy consumption, as significant resources are required to maintain precise operational conditions [3]. Even in cases where real-time closed loop feedback control is implemented to account for variability, the reliance on extensive sensor networks and rapid data processing can introduce prohibitive costs and practical limitations. Furthermore, unaccounted uncertainties can lead to deviations in key performance indicators (KPIs), increasing the likelihood of batch failures and product inconsistencies.

To address these challenges, robust optimisation techniques have been widely explored in the literature. One commonly employed approach is stochastic optimisation, which leverages probability distributions to model uncertainties and has been successfully applied in

complex, non-linear systems [4]. A particularly effective subset of stochastic optimisation is scenario tree optimisation, which transforms probabilistic problems into a structured deterministic framework by propagating uncertainty across different realisations of a process [5].

An emerging alternative to traditional set-point-based control is operational space control, which shifts the focus from maintaining rigid state profiles to defining feasible operational spaces within which a process can be adjusted [6]. This approach has found use in the chemical and pharmaceutical sectors, where it is often referred to as design space identification. For instance, [6] demonstrated the effectiveness of operational space methodologies in the temperature control of a fed-batch bioreactor under uncertainty, ensuring ethanol production constraints were met despite process variability. Such methodologies provide greater flexibility and adaptability than conventional set-point control, making them well-suited for processes characterised by uncertainty and dynamic variability [7].

Despite its advantages, current operational space methodologies still face notable challenges. Existing approaches often limit the consideration of uncertainty to parameter variations alone, overlook optimality in favour of robustness, and rely on computationally expensive sampling techniques. Moreover, there has been little research into the systematic identification of multiple feasible operational spaces for a given process, despite the potential benefits of having multiple viable operating regions. Notably, operational space control has yet to be applied in formulation industries, where the need for flexible quality control and real-time process monitoring is particularly pronounced.

In this paper, we address these gaps by proposing a novel scenario tree optimisation framework that integrates flexible operational spaces with dynamic optimisation. This framework not only enables the identification of multiple optimal and flexible operational regions but also enhances product quality control in a manner that is useful to real-world manufacturing constraints. Additionally, we present the first case study applying operational space methodologies to formulation processes, demonstrating the practical benefits of this approach in an industrial setting.

METHODOLOGY

Operational spaces can generally be categorised into three key classifications. The feasible space represents the multidimensional range of operating conditions that satisfy all process constraints. Within this, the flexible space forms a subset that is not only feasible but also resilient to uncertainties. Lastly, the optimal space is another subset of the feasible space where operating conditions are selected to maximise performance according to a predefined objective. In this study, we introduce a novel methodology to systematically identify the intersection of the flexible and optimal spaces, ensuring that the resulting solution space consists exclusively of operating conditions that are both robust to uncertainty and optimal in performance.

Additionally, as multiple distinct optimal operating conditions may exist, we seek to distinguish and characterise separate optimal regions within the identified design space. Each region is defined by a unique optimal state profile—or a set of profiles if multiple state variables are involved—along with its corresponding operational boundaries. In this work, we utilise an interval-based representation, where operating spaces are defined by upper and lower limits on the identified optimal state profiles. The overall methodology can be summarised into 4 steps, which are shown in Figure 1.

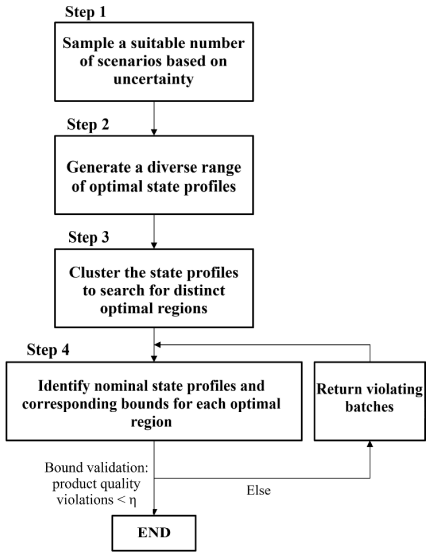

Figure 1. Schematic showing the general framework proposed in this study.

General Problem Formulation

We consider a mathematical model that captures the dynamics of the process, where state variables are categorised into two distinct groups: (i) Flexible state variables, denoted as $\dot{\boldsymbol{x}}_{flexible}(t_j) \in \mathbb{R}^{n_{flexible}}$, represent variables that can be directly adjusted through control inputs. Here, t_j indicates a specific time point within the operational time horizon. (ii) Dependent state variables, represented as $\dot{\boldsymbol{x}}_{dept}(t_j) \in \mathbb{R}^{n_{dept}}$, are those influenced by both control inputs and flexible state variables but cannot be directly regulated. The process dynamics are described by the following system of differential equations:

$$\dot{\boldsymbol{x}}_{flexible}(t) = \boldsymbol{F}_{flexible}(t, \boldsymbol{x}_{flexible}(t), \boldsymbol{\theta}, \boldsymbol{\xi}, \boldsymbol{u}(t)) \quad (1a)$$

$$\dot{\boldsymbol{x}}_{dept}(t) = \boldsymbol{F}_{dept}(t, \boldsymbol{x}_{dept}(t), \boldsymbol{x}_{flexible}(t), \boldsymbol{\theta}, \boldsymbol{\xi}) \quad (1b)$$

Where $\boldsymbol{u}(t_j) \in \mathbb{R}^m$ represents the vector of control inputs, $\boldsymbol{\theta} \in \mathbb{R}^p$ is the vector of fixed parameters, and $\boldsymbol{\xi} \in \mathbb{R}^r$ denotes the vector of uncertain parameters. Each source of uncertainty, ξ_i for $i = 1 \cdots r$, is modelled as a Gaussian-distributed random variable, with its mean set to the nominal parameter value, and its variance reflecting expected variability. Both parameters are assumed to be known.

The goal of this study is to determine a flexible, optimal, and practical operational space for $\boldsymbol{x}_{flexible}(t_j)$ ensuring that key performance indicators (KPIs), such as product quality, are consistently met while maximising process efficiency despite the presence of uncertainties. Herein, the term operational space will be used to refer specifically to the identified flexible state space of $\boldsymbol{x}_{flexible}(t_j)$.

Step 1: Sampling Uncertainty

We utilise scenario tree analysis, as discussed in Section 1, to capture the potential range of uncertainties encountered during processing. The full scenario tree is constructed by sampling each uncertainty source from its respective distribution, with a detailed description available in [8]. It is crucial to ensure that uncertainty is well-represented to develop a robust control strategy. Therefore, selecting a sufficient number of uncertainty samples is needed. However, this must be balanced against the increased computational cost associated with expanding the scenario tree. Once the scenario tree is established, all optimisation strategies are executed across the entire tree, ensuring that any imposed constraints are met under all considered uncertainty scenarios. An important note to consider is the computational expense of the methodology, which is largely dependent on the system under study. For high dimensional and complex systems, it should be encouraged to explore parallelisation, high performance computing alongside scenario reduction methods.

Step 2: Filling out the Optimal Region

Since multiple optimal state profiles of $\boldsymbol{x}_{flexible}(t)$ can satisfy process constraints while ensuring KPIs remain within specification, Step 2 (illustrated in Figure 1) focuses on refining the broad process design space. The goal is to identify promising operational regions that likely contain the majority of optimal state profiles of $\boldsymbol{x}_{flexible}(t)$. When successfully designed, these optimal operational regions should consist primarily—if not entirely—of state trajectories that adhere to a predefined standard of process efficiency while respecting constraints under all uncertainties represented in the scenario tree. Specifically, for each set of optimal state profiles, the objective is to minimise a process cost C_{avg}, which is computed as the average cost across all scenarios in the scenario tree, while ensuring that the calculated KPI remains within the specified range and close to its target value as defined in the PFD.

The operational time horizon is discretised into N intervals. To simplify control efforts, we assume that $\boldsymbol{x}_{flexible}(t)$ remains constant within each interval, meaning it follows a piecewise constant representation ($\boldsymbol{x}_{flexible}(t) = \boldsymbol{x}_k^{flexible}$, for $t \in [t_k, t_{k+1})$ and $k = 0 \cdots N-1$), where $t_k = k\Delta t$ and $\Delta t = {}^{t_f}/_{N}$. Furthermore, due to physical constraints on control actions $\boldsymbol{u}(t)$, the flexible state variables are also bounded within a predefined range, $[\underline{\boldsymbol{x}}_k^{flexible}, \overline{\boldsymbol{x}}_k^{flexible}]$ for $k = 0 \cdots N-1$. The process is also subject to constraints, $\boldsymbol{g}(\boldsymbol{x}_{k,s}^{dept}, \boldsymbol{x}_k^{flexible})$ for $s = 1 \cdots S$, where S represents the number of uncertain scenarios in the scenario tree. Additionally, it is assumed that the initial state $\boldsymbol{x}_0^{dept}$ is known. With these considerations, the optimisation problem is defined to determine the optimal state trajectories of $\boldsymbol{x}_{flexible}$.

$$min_{x_k^{flexible}, k=0,\ldots,N-1} \lambda_1 \cdot obj_1 + \lambda_2 \cdot C_{avg} \quad (2)$$

$$s.t.$$

$$for\ k = 0, \ldots, N-1, s = 1, \ldots, S,$$

$$obj_1 = (1/S) \sum_{s=1}^{S} \left(y_{KPI,s} - y_{KPI,T}\right)^2$$

$$C_{avg} = (1/S) \sum_{s=1}^{S} C_s$$

$$y_{KPI,s} = h\left(\boldsymbol{x}_{k,s}^{dept}, \boldsymbol{x}_k^{flexible}\right)$$

$$\boldsymbol{x}_{k+1,s}^{dept} = \boldsymbol{f}_{dept}\left(\Delta t, \boldsymbol{x}_k^{dept,s}, \boldsymbol{x}_k^{flexible}, \boldsymbol{\theta}, \boldsymbol{\xi}_s\right)$$

$$\boldsymbol{g}\left(\boldsymbol{x}_k^{dept,s}, \boldsymbol{x}_k^{flexible}\right) \leq 0$$

$$\boldsymbol{x}_0^{dept} = \boldsymbol{x}^{dept}(0)$$

$$\underline{\boldsymbol{x}}_k^{flexible} \leq \boldsymbol{x}_k^{flexible} \leq \overline{\boldsymbol{x}}_k^{flexible}, \underline{y}_{KPI} \leq y_{KPI,s} \leq \overline{y}_{KPI}$$

Here, λ_1 and λ_2 are weighting parameters assigned to each objective. obj_1 represents the average sum-of-squared deviations from the target KPIs across all scenarios, while C_s denotes the process cost for each scenario. The function $h(\cdot)$ describes the transformation between process states and their corresponding KPIs, where $y_{KPI,s}$ and $y_{KPI,T}$ represent the KPI value for Scenario s and the target KPI value, respectively. The term $\boldsymbol{f}_{dept}(\cdot)$ accounts for the numerical integration of the dependent state variables. $\boldsymbol{g}(\cdot)$ is the process inequality constraints.

To obtain a diverse set of optimal state trajectories and explore a broader operational space, the optimisation of Problem 2 is initially performed. Once this is complete, additional optimal state profiles can be identified by re-optimising the problem with an additional penalty function, p, introduced into the objective function. The penalty used may be:

$$p = \lambda_3 \cdot \sum_{d=1}^{D_{curr}} \sum_{j=1}^{n_{flexible}} \sum_{k=0}^{N-1} \left(\frac{\left(x_{flexible,j,k} - x^*_{flexible,j,k,d}\right)}{\Delta \bar{x}_{flexible,j,k}} \right) \quad (3)$$

Here, $\boldsymbol{\lambda_3}$ serves as the weighting parameter that regulates the strength of the penalty function. Higher values encourage greater variation among solutions, thereby facilitating the identification of more distinct optimal regions. The term D_{curr} denotes the number of previous optimisation iterations, which increases as the number of iterations does. Within this framework, $x^*_{flexible,j,k,d}$ represents the discretised optimal state value from an already identified trajectory, whereas $x_{flexible,j,k}$ corresponds to the state value in the current optimisation. To ensure comparability across variables with different scales, the term $\Delta\bar{x}_{flexible,j,k}$ represents the maximum range of $x_{flexible,j,k}$ across previously identified trajectories. By applying this iterative approach, and with a sufficiently large number of iterations D_{max} , one can systematically explore the entire design space to uncover a broad set of high-quality optimal state profiles that remain feasible under uncertainty.

Step 3: Clustering Optimal Regions

After completing Step 2, multiple operational spaces may emerge. To systematically identify and characterise these spaces, clustering algorithms are employed. Given that clustering is an unsupervised learning approach, it is crucial to validate the results by applying different clustering methods and analysing the resulting cluster characteristics. This ensures a clear distinction between solutions and assists to assess variations in their behaviours. In this work, several algorithms were used and compared in order to ensure consistent results for the recommended number of clusters. These are k-means, DBSCAN, and spectral clustering [9].

Step 4: Nominal State and Bound Estimation Strategy

In Steps 2 and 3 (as shown in Figure 1), estimations for a set of distinct optimal operational regions are made. The next step involves refining these regions by determining the nominal state profiles for each region, as well as the upper and lower bounds for each flexible state variable. An optimal operational region for a particular flexible state variable is characterised by its nominal profile and associated bounds, where staying within these bounds provides feasibility under the given uncertainties.

The nominal profiles, which represent the optimised state variable set-points at various stages of the process, are identified through a dynamic optimisation approach, as described in Problem 2. At this point, the search space is limited to the clustered region defined in Step 3. This ensures the solution remains within the appropriate cluster. Consequently, the bounds in Problem 2, $\underline{\boldsymbol{x}}_k^{flexible}$ and $\overline{\boldsymbol{x}}_{\mathrm{k}}^{flexible}$, are adjusted to reflect the specific characteristics of the cluster. Once the nominal profiles are determined, a two-step algorithm is proposed to independently find the upper and lower bounds, maximising the distance between them while still adhering to process constraints. The optimisation strategy for determining the lower bound is shown in Equation 4.

$$\max_{\substack{x_k^{flexible,lb} \\ k=0\cdots N-1}} \min_{j=1}^{(n_{flexible})} \min_{k=1}^{(N-1)} \underline{w}_{j,k} \cdot \left(x_{j,k}^{flexible,nominal} - x_{j,k}^{flexible,lb}\right)$$

$$s.t. \tag{4}$$

$$\underline{w}_{j,k} = \frac{1}{x_{j,k}^{flexible,nominal} - \underline{x}_{j,k}^{flexible}}$$

$$y_{KPI,s} = h\left(\boldsymbol{x}_{k,s}^{dept}, \boldsymbol{x}_k^{flexible}\right)$$

$$\boldsymbol{x}_{k+1,s}^{dept} = \boldsymbol{f}_{dept}\left(\Delta t, \boldsymbol{x}_{k,s}^{dept}, \boldsymbol{x}_k^{flexible,lb}, \boldsymbol{\theta}, \boldsymbol{\xi}_s\right)$$

$$\boldsymbol{g}\left(\boldsymbol{x}_{k,s}^{dept}, \boldsymbol{x}_k^{flexible,lb}\right) \leq 0$$

$$\boldsymbol{x}_0^{dept} = \boldsymbol{x}^{dept}(0)$$

$$\underline{\boldsymbol{x}}_k^{flexible} \leq \boldsymbol{x}_k^{flexible,lb} \leq \boldsymbol{x}_k^{flexible,nominal}, \underline{y}_{KPI} \leq y_{KPI,s} \leq \overline{y}_{KPI}$$

Problem 4 is designed to maximise the minimum distance between the nominal flexible state, $x_{j,k}^{flexible,nominal}$, and the lower bound of the flexible state, $x_{j,k}^{flexible,lb}$, across all flexible state variables and time steps. The normalisation parameter, $\underline{w}_{j,k}$, is used to standardise the influence of different flexible states on the objective function. By formulating the objective this way, the goal is to spread the bounds as evenly as possible across the entire trajectory for each flexible state variable. This reduces the need for highly precise set-point control at any given time step.

This optimisation strategy can be repeated for the upper bound to provide the full operational region where control of the design variables can be relaxed but achieve good process performance and required specifications. As the two-step algorithm determines the upper and lower bounds independently, each bound is ensured to meet the constraints on its own. However, this does not guarantee that all state profiles sampled within these bounds will adhere to the constraints. Therefore, it is crucial to validate these bounds by randomly sampling state profiles within them and identifying instances where constraints are violated. Once these violating samples are recorded, they are reintroduced into the framework by incorporating a penalty function into the objective functions of Equations (4) and (5). This penalty function serves to narrow the bounds, ensuring that future state profiles do not violate the constraints. The penalty function may take many forms dependant on the study, but one must consider its practicality against its conservativeness.

CASE STUDY

To illustrate the effectiveness of the proposed framework, an in-silico case study has been developed using a dynamic model designed to simulate a real-world industrial formulation process. A simplified schematic of the primary mixing unit is presented in Figure 2. This case study focuses on the production of a multiphase, non-Newtonian liquid formulation via a batch mixing process where the process flow diagram (PFD) is characterised by a sequence of ingredient additions, alongside key processing such as temperature and shear rate. Due to the complex nature of multiphase mixing mechanisms, the product KPI is inherently challenging to control and cannot be measured in real-time. As a result, defining a robust operational space that ensures both process flexibility and consistent product quality is essential. Furthermore, it is desired to reduce operational expense and improve the sustainability of the process through reducing the batch cycle time (i.e., the process cost).

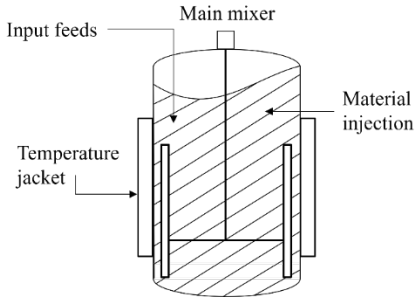

Figure 2. Diagram of the batch mixing unit for which the case study is based on.

Within this study, both the sequence of ingredient additions and the final ingredient ratio and mass are predefined by established protocols. As a result, the selection of flexible state variables is limited to standard processing parameters such as shear rate, pressure, temperature, and flowrate. For this investigation, two process parameters are chosen, along with an additional variable representing the timing of ingredient additions, leading to a total of three distinct types of flexible state variables. A mechanistic model exists to describe the dynamic mixing process with high accuracy, a full description of which can be found in [10]. In this model, there exists a set of 5 key ingredient concentrations (dependent states), determined dynamically through 3 material transformation equations, which influence the product quality. Furthermore, there are 3 flexible state variables used to control the process, and in total, there are 14 model parameters which were parameterised. The 3 flexible state variables were each discretised into 5 decision variables for the purpose of solving the optimal control problem (i.e., a total of 15 decision variables). The 3 flexible state variables will henceforth be referred to as Process Parameters 1, 2 and 3.

The primary challenges in this case study stems from the difficulty in achieving the desired end-product quality, which is influenced by various process uncertainties typically encountered in standard operations. These uncertainties were categorised into three sources. The first being variations in the input feed composition, which are reflected in the estimated model parameters. The second source is human error, primarily introduced through inconsistencies in precisely following the scheduled timing for ingredient additions. The third source is system control error, which involves deviations in state variables from their set-point values. The uncertainty levels for these variables were assumed to be 10%, 20%, and 5%, respectively. Additionally, 100 uncertain scenarios were considered in the assembly of the scenario tree.

RESULTS AND DISCUSSION

The methodology outlined in Section 2 was fully implemented, resulting in the identification of 40 optimal set-points during step 2. In Step 3, the analysis revealed the presence of two distinct clusters, each associated with separate state profiles which were both carried forth for Step 4. From application of Step 4, the initial nominal state profiles and corresponding bounds for Process Parameters 1 and 2 in each cluster were determined as shown in Figures 3 (initial bounds) and 4 (refined bounds).

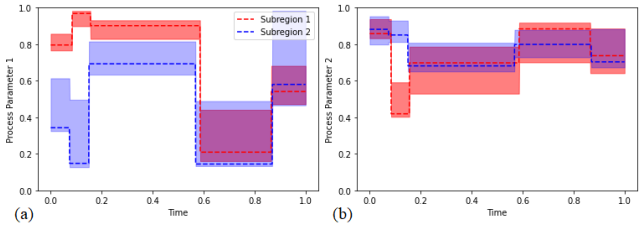

Figure 3. Normalised state profiles and operational region for Process Parameters 1(a) and 2(b) for each of the clusters identified before bound refinement

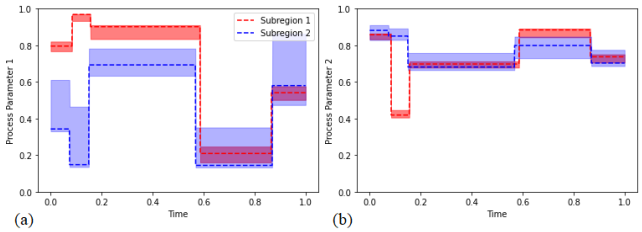

Figure 4. Normalised state profiles and operational region for Process Parameters 1(a) and 2(b) for each of the clusters identified after bound refinement.

To validate the initial bounds for both clusters, 1000 state trajectories were randomly sampled from within the optimal operational regions, across 100 unseen uncertain scenarios (i.e., 10^5 tests). To compare the performance, the batch failure rate is defined: this is the fraction of the

test batches that encounter a product quality violation. After validation of the initial bounds (Figure 3), the results showed that Cluster 1 and 2 had a batch failure rate of 0.9% and 0.1%, respectively, suggesting that the initial bounds are reasonably robust to uncertainties.

When the bounds were refined (Figure 4), the batch failure rates dropped significantly to 0% and 0.009% for Clusters 1 and 2, respectively. However, it is immediately noticed that the refined operational area of Cluster 2 is much greater than that of Cluster 1. Specifically, Cluster 1's refined operational areas are 67.1% and 59.2% smaller for Process Parameters 1 and 2, respectively. Using these results, we can conclude that although it may be possible to achieve a 0% batch failure rate, it may be more practical to permit a small batch failure rate in order to largely improve flexibility in the operational area.

Overall, this case study demonstrates the framework's capacity to identify multiple distinct optimal regions, each offering operational areas that are practically resilient to uncertainties. Additionally, both identified regions led to a significant reduction in batch time compared to the existing set-point control approach used for the system, achieving a 38.6% decrease in both cases. After a thorough evaluation of each operational region's performance, it is likely that Region 2 would be recommended for execution, given its greater operational flexibility to Region 1.

CONCLUSION

In conclusion, operational space design provides an innovative approach for integrating uncertainties into the development of robust control strategies, ensuring that key process constraints are reliably met. By combining flexibility with optimality, this approach enables the creation of control strategies that are both reliable and high-performing. A significant advantage over traditional set-point control is the increased operability, which allows processes to operate within broader ranges instead of being constrained to strict set-point conditions. Additionally, the systematic identification of various operating regions within the entire optimal space offers a major benefit over traditional set-point control, which may overlook the existence of such regions. This methodology not only aids in designing robust controls but also provides valuable insights into how processes can be operated, helping operators identify areas where the process may be more stable and easier to control.

REFERENCES

1. A. Hicks *et al.*, "A two-step multivariate statistical learning approach for batch process soft sensing," *Digital Chemical Engineering*, vol. 1, p. 100003, Dec. 2021.
2. H. Efheij, A. Albagul, and N. A. Albraiki, "Comparison of Model Predictive Control and PID Controller in Real Time Process Control System," *19th International Conference on Sciences and Techniques of Automatic Control and Computer Engineering, STA 2019*, pp. 64–69, May 2019.
3. H. S. Asad, R. K. K. Yuen, and G. Huang, "Multiplexed real-time optimization of HVAC systems with enhanced control stability," *Appl Energy*, vol. 187, pp. 640–651, Feb. 2017.
4. Q. P. Zheng, J. Wang, and A. L. Liu, "Stochastic Optimization for Unit Commitment - A Review," *IEEE Transactions on Power Systems*, vol. 30, no. 4, pp. 1913–1924, Jul. 2015.
5. J. Silvente, L. G. Papageorgiou, and V. Dua, "Scenario tree reduction for optimisation under uncertainty using sensitivity analysis," *Comput Chem Eng*, vol. 125, pp. 449–459, Jun. 2019.
6. T. Forster, D. Vázquez, I. F. Moreno-Palancas, and G. Guillén-Gosálbez, "Algebraic surrogate-based flexibility analysis of process units with complicating process constraints," *Comput Chem Eng*, vol. 184, p. 108630, May 2024.
7. J. Djuris and Z. Djuric, "Modeling in the quality by design environment: Regulatory requirements and recommendations for design space and control strategy appointment," *Int J Pharm*, vol. 533, no. 2, pp. 346–356, Nov. 2017.
8. T. Homem-de-Mello and G. Bayraksan, "Monte Carlo sampling-based methods for stochastic optimization," *Surveys in Operations Research and Management Science*, vol. 19, no. 1, pp. 56–85, Jan. 2014.
9. N. Murugesan, I. Cho, and C. Tortora, "Benchmarking in Cluster Analysis: A Study on Spectral Clustering, DBSCAN, and K-Means," *Studies in Classification, Data Analysis, and Knowledge Organization*, vol. 5, pp. 175–185, 2021.
10. A. W. Rogers *et al.*, "Integrating knowledge-guided symbolic regression and model-based design of experiments to automate process flow diagram development," May 2024.